PHYSICAL REVIEW E **76**, 015202(R) (2007)

Fractal conductance fluctuations of classical origin

H. Hennig,[1,2] R. Fleischmann,[1,2] L. Hufnagel,[3] and T. Geisel[1,2]
[1]*Max Planck Institute for Dynamics and Self-Organization, 37073 Göttingen, Germany*
[2]*Department of Physics, University of Göttingen, Göttingen, Germany*
[3]*Kavli Institute for Theoretical Physics, University of California, Santa Barbara, California 93106, USA*
(Received 21 December 2006; published 16 July 2007)

In mesoscopic systems, conductance fluctuations are a sensitive probe of electron dynamics and chaotic phenomena. We show that the conductance of a purely classical chaotic system, with either fully chaotic or mixed phase space, generically exhibits fractal conductance fluctuations unrelated to quantum interference. This might explain the unexpected dependence of the fractal dimension of the conductance curves on the (quantum) phase breaking length observed in experiments on semiconductor quantum dots.

DOI: 10.1103/PhysRevE.76.015202 PACS number(s): 05.45.Df, 73.23.Ad, 05.60.Cd

A prominent feature of transport in mesoscopic systems is that the conductance as a function of an external parameter (e.g., a gate voltage or a magnetic field) shows reproducible fluctuations caused by quantum interference [1]. A prediction from semiclassical theory that inspired a number of both theoretical and experimental works in the fields of mesoscopic systems and quantum chaos was that, in chaotic systems with a mixed phase space, these fluctuations would result in fractal conductance curves [2,3]. Such fractal conductance fluctuations (FCFs) have since been confirmed in gold nanowires and in mesoscopic semiconductor billiards in various experiments [4–8]. In addition, FCFs have more recently been predicted to occur in strongly dynamically localized [9] and in diffusive systems [10]. Due to the quantum nature of the FCFs, it came as a surprise when recent experiments indicated that decoherence does not destroy the fractal nature of the conductance curve, but only changes its fractal dimension [11,12]. In the present Rapid Communication, we show that the conductance of purely classical (i.e., incoherent) low-dimensional Hamiltonian systems very fundamentally exhibits fractal fluctuations, as long as transport is at least partially conducted by chaotic dynamics. Thus, mixed phase space systems and fully chaotic systems alike generally show FCFs with a fractal dimension that is determined analytically. We show that it is governed by fundamental properties of chaotic dynamics.

In a disordered mesoscopic conductor—which is smaller than the phase coherence length of the charge carriers but large compared to the average impurity spacing—the transmission is the result of the interference of many different, multiply scattered, and complicated paths through the system. As these paths are typically very long compared to the wavelength of the charge carriers, the accumulated phase along a path changes basically randomly when an external parameter, such as the energy or the magnetic field, is varied. This results in a random interference pattern, i.e., reproducible fluctuations in the conductance of a universal magnitude on the order of $2e^2/h$, the so-called universal conductance fluctuations. For a review, see [13] or [14]. The role of disorder in providing a distribution of random phases can as well be taken by chaos. Thus ballistic mesoscopic cavities like quantum dots in high-mobility two-dimensional electron gases that form *chaotic billiards* show the same universal fluctuations [1,15,16]. If the average of the *phase gain* accumulated on the different paths traversing the system exists, the conductance curves are smooth on parameter scales that correspond to a change of the average phase gain on the order of and smaller than the wavelength of the carriers. In systems with mixed phase space, where chaotic and regular motion coexist, this phase gain, however, is typically algebraically distributed, and an average phase gain does not exist (neglecting the finiteness of the coherence length and assuming the semiclassical limit $\hbar_{eff} \to 0$; the role of the finite $\hbar_{eff}$ is discussed in [3]). Therefore, as shown in [2], the conductance curve of such a system fluctuates on all parameter scales and forms a fractal. The fractal dimension D is connected to the exponent γ of the algebraic distribution of phase gains by $D=2-\gamma/2$.

Experiments on quantum dots that study the dependence of the conductance fluctuations on several system parameters like size and temperature seem to partly contradict the semiclassical theory of fractal scaling [11,12]. Namely, it was found that with decreasing coherence length the scaling region over which the fractal was observed did not shrink—as would be expected from the semiclassical arguments—but that the fractal dimension changed. An implicit assumption of the semiclassical theory is that the classical dynamics remains unchanged as the external parameter is varied, and thus only phase changes are relevant. In most experimental setups, however, the classical phase space changes with variation of the control parameter. In this Rapid Communication, we show that the classical chaotic dynamics itself already leads to fractal conductance curves. Moreover, from this it follows that, even on very small parameter scales, the fluctuations due to changes in the classical dynamics are important. In general, the conductance curve is a superposition of two fractals: one originating in interference, which is suppressed by decoherence to reveal the fractal fluctuations reflecting the changes in the classical phase space structure. In addition, we predict that FCFs are observable not only in systems with a mixed phase space, but in purely chaotic systems.

As a starting point of our investigation and to connect it to the experiments, we numerically study the classical conductance through a rectangular (hard wall) and a stadium billiard (soft wall) as a function of magnetic field, as shown in Fig. 1 (Throughout this Rapid Communication, we will study the transmission, which, in accordance with the Landauer theory

 ©2007 The American Physical Society

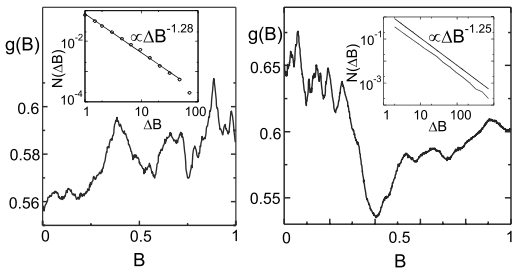

FIG. 1. Classical conductance $g(B)$ through a stadium (left, geometry as in Ref. [5]) and a square billiard (right, geometry as in Ref. [11]) versus magnetic field B. Both fluctuating conductance curves are fractals (see insets and text). Their dimensions are $D \approx 1.28$ for the stadium and $D \approx 1.25$ for the square billiard. The fractal dimensions are in good agreement with experimental measurements [5,11].

of conductance, is proportional to the conductance; see, e.g., [17].) Note that not only the phase space of the stadium but also that of the rectangular billiard is mixed in the presence of a perpendicular magnetic field. In both cases, a modified version [18,19] of the box-counting analysis clearly reveals the fractal nature of the conductance curves. As the simulation is purely classical, the fractal scaling cannot be caused by interference effects. So what is the underlying mechanism for the fractality of the conductance curve, and how can we understand its dimension?

To study this mechanism in detail, we will, because of its numerical and conceptual advantages, analyze the transport in Chirikov's standard map [21–23]. This paradigmatic system shows all the richness of Hamiltonian chaos. And since—as will become apparent below—our theory relies only on very fundamental properties of chaotic systems, it is a natural choice as a model system. The standard map is defined by $\theta' = p + \theta$, $p' = p + K \sin \theta'$, with momentum p, angle θ, and the "nonlinearity parameter" K, which drives the dynamics from fully integrable ($K=0$) to fully chaotic ($K \gtrsim 7$). In between, the phase space is mixed. The standard map can be seen as the Poincaré surface of a conservative system of two degrees of freedom. As such, the map can by viewed as directly corresponding to the Poincaré map at the boundary of a chaotic ballistic cavity, connecting it conceptually with the experimental system. We introduce absorbing boundary conditions (see, e.g., Ref. [24]), i.e., when p exceeds (drops below) a maximum (minimum) threshold value, the particle is transmitted (reflected) and leaves the cavity. As can be seen right from the definition of the standard map, the envelope of the entry set (which is the phase space projection of the injection lead) is simply half a period of a sine function times K.

A trajectory entering the system eventually contributes to either the total transmission or reflection, and we mark the corresponding point in the entry set by a color code (transmission, red; reflection, blue). Chaotic dynamics, through its fundamental property of stretching and folding in phase space, leads to a lobe structure [see Fig. 2 bottom], which is typical for chaotic systems and not special to the standard map. The distribution of widths w of lobes exhibits a power law,

$$n(w) \propto w^{-\alpha}. \tag{1}$$

The lobe structure is translated into transmission by summing up the intersections of the transmission lobes along a horizontal line (see Fig. 2). A lobe of thickness w gives rise to a maximum contribution $\Delta T \propto w^{\beta}$. Variation of the external parameter K leads to a fractal transmission curve $T(K)$ with $D \approx 1.25$.

How does the fractal dimension depend on the power law distribution of lobe widths and the curvature of the lobes? With this aim, we study a random sequence of curve segments mimicking the intersection of consecutive lobes of widths w, distributed algebraically with exponent α, and curved as w^{β}. We define $X_i := \Sigma_{j=1}^{i} w_j$ and $T(X) = (-1)^i (X - X_i)^{\beta}$, $X_i < X \leqslant X_{i+1}$. An example of this curve of "random lobes" with $\alpha = 1.9$ and $\beta = \frac{1}{2}$ is shown in Fig. 3 (top). The box-counting analysis clearly reveals a fractal structure.

We further simplify the problem by replacing the lobes by a sequence of stripes of widths x with power law distribution $n(x) \propto x^{\alpha}$. Dispensing with the sign of the fluctuation, the transmission reads $T(X) = (X_{i+1} - X_i)^{\beta}$. This yields histogrammatic transmission curves $T(X)$ like the bottom curve of Fig. 3. As shown in the inset, the fractal dimension of the resulting transmission curve remains unchanged compared to the corresponding calculation with random lobes, within the precision of the box-counting analysis. Thus, the fractal dimension of the curve does not change noticeably when considering stripes instead of lobes, nor when neglecting the sign of each contribution, confirming the intuition that the fractal dimension depends only on the relative scaling, i.e., α and β, but not on the detailed form of the curve sections.

For these curves like the bottom one of Fig. 3 with $\alpha - \beta > 1$, we can give an analytical expression for the fractal dimension and then estimate the fractal dimension of the transmission curve in the standard map. We apply the box-counting method, which we therefore review briefly (see, e.g., [19] for a more detailed introduction). In this approach the fractal curve lying in an n-dimensional space is covered by an n-dimensional grid. Let the grid consist of boxes of length scale s. The box-counting dimension is then given by

$$D = -\lim_{s \to 0} \frac{\log N(s)}{\log s}, \tag{2}$$

where $N(s)$ is the number of nonempty boxes. For our problem, we divide $N(s)$ into three contributions $N(s) = n_a + n_b + n_c$, as schematically drawn in Fig. 4(a). The number n_a of vertically placed boxes [see mark (a)] covering contributions from stripes of widths $x > s$ reads

$$n_a(s) \propto \frac{1}{s} \int_s^{\infty} p(x) x^{\beta} dx \propto s^{-(\alpha - \beta)}. \tag{3}$$

Second, the number n_b of horizontally placed boxes covering horizontal contributions of stripes of widths larger than s [see Fig. 4(Ab)], is given by

$$n_b(s) = \frac{1}{s} \int_s^{\infty} p(x) x dx < \frac{1}{s} \int_0^{\infty} p(x) x dx. \tag{4}$$

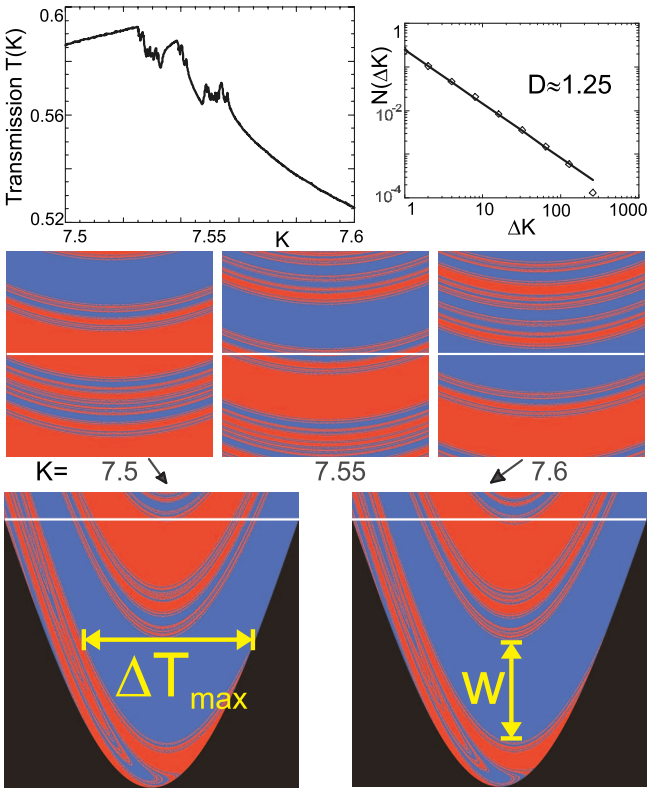

FIG. 2. (Color) How lobes translate into fluctuations. In the bottom row, the entry set of the standard map with absorbing boundary conditions at $\pm 3\pi$ for $K=7.5$ and 7.6, respectively, can be seen. The three pictures in the center row show the magnification of the central sections of the entry set for three different values of $K=7.5$, 7.55, and 7.6. The transmission $T(K)$ for $K=7.5-7.6$ [20] is shown in the top left picture. Note that a small change in K shifts the lobes vertically, but conserves the overall phase space structure, and that the largest fluctuations are caused by intersection with the apex of lobes. Starting from $K=7.5$, a large transmission lobe is cut by the horizontal line (see text), i.e., the transmission increases with K. In the same way, e.g., the fluctuations of $T(K)$ near $K=7.55$ can be understood. The box-counting analysis reveals a fractal structure (top right).

Hence n_b scales like s^{-1} and can be neglected in comparison to n_a, because $\alpha-\beta>1$. Finally, we determine an upper estimate for the number n_c of vertically placed boxes covering the contribution from stripes of widths $x \leqslant s$. The total length of these widths is $L(s)=\int_0^s p(x)x dx$; therefore $L(s)/s$ boxes are needed to cover the length. Inflating all *heights* of the stripes $x \leqslant s$ to the maximum possible size s^β [see Fig. 4(Ac)], we find

$$n_c(s) < [L(s)/s](s^\beta/s) \propto s^{-\alpha+\beta}. \tag{5}$$

Thus for $s \ll 1$ the dominant term is $n_a(s)$. With Eq. (2), $N(s)$ gives rise to the box-counting dimension [25]

$$D = -\lim_{s\to 0} \frac{\log s^{-\alpha+\beta}}{\log s} = \alpha - \beta. \tag{6}$$

To connect the analytical result with the calculations of the transmission of the open standard map, we numerically

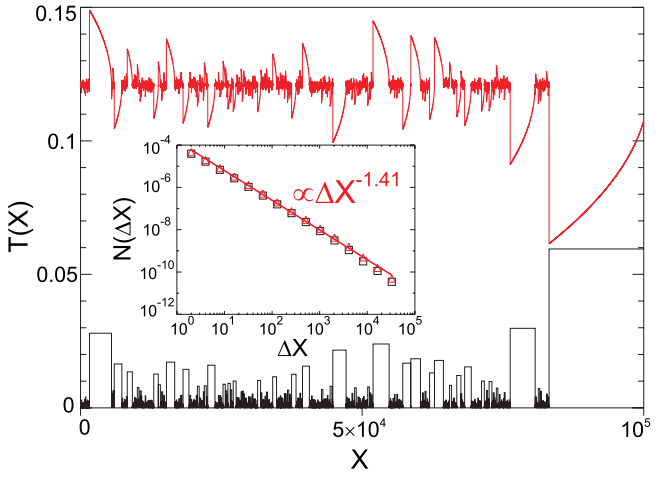

FIG. 3. (Color) Transmission $T(X)$ for lobes (red upper curve, shifted along the y axis for clarity) and stripes (black lower curve) for one and the same random distribution with $\alpha=1.9$, $\beta=0.5$. The inset shows the box-counting analysis for the upper (red triangles) and lower (black squares) transmission curves. The regression line is drawn for the upper curve, whose fractal dimension is 1.41.

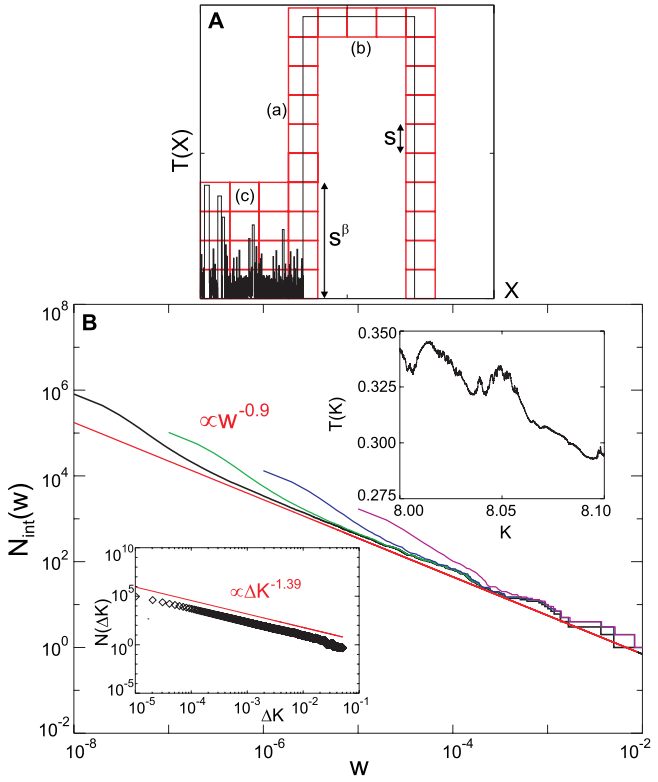

FIG. 4. (Color) (A) Schematic transmission according to Fig. 3 (bottom), covered with boxes of size s. There are three contributions marked (a)–(c). (B) Total number $N_{int}(w)=\int_w^\infty n(w')dw'$ of lobes (for the open standard map with $|p|<4\pi$) of width larger than w on a double-logarithmic scale. The four curves show estimates for increasing resolution $w_{\min}=10^{-5}$(pink)-10^{-8}(black). The curves clearly approach a power law corresponding to $n(w)\propto w^{-1.9}$. The insets show the transmission curve $T(K)$ for values $K=8.0-8.1$ calculated from 2×10^{13} trajectories, and its box-counting dimension.

estimate the distribution of lobe widths in the entry set for $K=8$, finding $\alpha \approx 1.9$, as shown in Fig. 4(B). Together with $\beta=\frac{1}{2}$, corresponding to first-order Taylor expansion of the cosine function, Eq. (6) predicts a fractal dimension $D \approx 1.4$. Direct analysis of the transmission curve [see insets of Fig. 4(B)] yields a fractal dimension $D \approx 1.39$, in good agreement with the expected value.

How can a power law distribution of lobe widths emerge in a fully chaotic open system? One might rather expect to find an exponential distribution of lobes in a fully chaotic system. To see why the distribution is algebraic, however, let us examine the simplest case of an open chaotic area-preserving map, the dynamics of which is governed by a single, positive homogeneous Lyapunov exponent λ. In each iteration, phase space structures are stretched in one direction by $\exp(\lambda)$, shrunk by $\exp(-\lambda)$ in the other, and then folded back. The entry set of the open system is thus stretched into lobes of decaying width $w(t_i) \propto \exp(-\lambda t_i)$. The phase space volume flux out of the system decays exponentially, as is typical for a fully chaotic phase space, i.e., $\Gamma(t_i) \propto \exp(-t_i/\tau)$, with (mean) dwell time τ. The area $\Gamma(t_i)\Delta t$ is the fraction of the exit set that leaves the system at time t_i. With $t_i(w) \propto -\ln(w)/\lambda$, the number of lobes of width w in the exit set is [26]

$$\mathcal{N}(w) = \frac{\Gamma(t_i(w))\Delta t}{w} \propto \frac{1}{w} \exp\left(\frac{(\ln(w)}{\lambda \tau}\right) = w^{1/\lambda\tau - 1}.$$

This suggests that the power law distribution of lobe widths is a generic property even for fully chaotic systems. A quantitative expression for the exponent, however, is not as easy to derive, as, e.g., the Lyapunov exponent for the standard map is not homogeneous.

In conclusion, we have shown that transport through chaotic systems due to the typical lobe structure of the phase space in general produces fractal conductance curves, where the fractal dimension reflects the distribution of lobes in the exit and/or entry set. In contrast to the semiclassical effect, the size of the fluctuations is not universal, but depends on specific system parameters. Due to the fractal nature of the classical conductance, however, there is no parameter scale that separates coherent and incoherent fluctuations.

[1] C. M. Marcus *et al.*, Phys. Rev. Lett. **69**, 506 (1992).
[2] R. Ketzmerick, Phys. Rev. B **54**, 10841 (1996).
[3] L. Hufnagel, R. Ketzmerick, and M. Weiss, Europhys. Lett. **54**, 703 (2001).
[4] H. Hegger *et al.*, Phys. Rev. Lett. **77**, 3885 (1996).
[5] A. S. Sachrajda *et al.*, Phys. Rev. Lett. **80**, 1948 (1998).
[6] A. P. Micolich *et al.*, J. Phys.: Condens. Matter **10**, 1339 (1998).
[7] Y. Ochiai *et al.*, Semicond. Sci. Technol. **13**, A15 (1998).
[8] Y. Takagaki, Phys. Rev. B **62**, 10255 (2000).
[9] I. Guarneri and M. Terraneo, Phys. Rev. E **65**, 015203(R) (2001).
[10] F. A. Pinheiro and C. H. Lewenkopf, Braz. J. Phys. **36**, 379 (2006).
[11] A. P. Micolich *et al.*, Phys. Rev. Lett. **87**, 036802 (2001).
[12] A. P. Micolich *et al.*, Physica E (Amsterdam) **13**, 683 (2002).
[13] *Introduction to Mesoscopic Physics*, edited by Y. Imry (Oxford University Press, Oxford, 2002).
[14] *Transport in Nanostructures*, edited by D. K. Ferry and S. M. Goodnick (Cambridge University Press, Cambridge, U.K., 2005).
[15] R. A. Jalabert, H. U. Baranger, and A. D. Stone, Phys. Rev. Lett. **65**, 2442 (1990).
[16] H. U. Baranger, R. A. Jalabert, and A. D. Stone, Chaos **3**, 665 (1993).
[17] *Electronic Transport in Mesoscopic Systems*, edited by S. Datta (Cambridge University Press, Cambridge, U.K., 1995).
[18] Throughout this paper, in order to determine the fractal dimension of a given 2D curve $T(\Delta k)$, we used the so-called variation method, i.e., we calculated $N(\Delta k)=\langle \max[T(\Delta k)] - \min[T(\Delta k)]\rangle$, where $N(\Delta k) \propto (\Delta k)^{-D}$ for a fractal curve of dimension D.
[19] *Fractals, Scaling and Growth far from Equilibrium*, edited by P. Meakin (Cambridge University Press, Cambridge, U.K., 1998).
[20] The range of the K value is close to the first fundamental accelerator mode regime which terminates at $K=7.45$. However, trajectories in remaining accelerator mode islands will exit the phase space quickly, and do not affect the ensuing statistics.
[21] B. V. Chirikov, Phys. Rep. **52**, 263 (1979).
[22] S. Fishman, D. R. Grempel, and R. E. Prange, Phys. Rev. Lett. **49**, 509 (1982).
[23] A. Altland and M. R. Zirnbauer, Phys. Rev. Lett. **77**, 4536 (1996).
[24] P. Jacquod and E. V. Sukhorukov, Phys. Rev. Lett. **92**, 116801 (2004).
[25] A numerical calculation of the fractal dimension of transmission curves based on random lobes for various pairs of (α, β) shows good agreement with the analytical result for $\alpha - \beta \gtrsim 1.2$.
[26] We showed the argument for the exit set and not for the entry set for the sake of clarity. A corresponding relation for the algebraic distribution of lobe widths in the entry set can be derived easily by studying the time-reversed map, which again is a chaotic map with the same properties.